Supporting Information:

Enrichment of large-diameter semiconducting SWCNTs by polyfluorene extraction for high network density thin film transistors

Jianfu Ding*[1], Zhao Li[1], Jacques Lefebvre[2], Fuyong Cheng[3], Girjesh Dubey[3,6], Shan Zou[4], Paul Finnie[2], Amy Hrdina[3], Ludmila Scoles[5], Gregory Lopinski[4], Christopher T. Kingston[3], Benoit Simard[3] and Patrick R. L. Malenfant*[2]

[1] [2] [3] Security and Disruptive Technologies Portfolio, National Research Council Canada, [1] M-12, 1200 Montreal Road, Ottawa, Ontario, K1A 0R6, Canada, [2] M-50, 1200 Montreal Road, Ottawa, Ontario, K1A 0R6, Canada, [3] 100 Sussex Drive, Ottawa, Ontario, K1A 0R6, Canada; [4] Measurement Science and Standards, 100 Sussex Drive, Ottawa, Ontario, K1A 0R6, Canada; [5] Energy, Mining and Environment Portfolio, National Research Council Canada, M-12, 1200 Montreal Road, Ottawa, Ontario, K1A 0R6, Canada. [6] Current address: Max-Planck-Institute for Solid State Research, Heisenbergstraße 1, 70569, Stuttgart, Germany.

List of Content:

1. Polymer synthesis and thermal property:[1]

1-1. 2,7-dibromo-9,9-dialkylflourene (for C10, C12, and C14): 2,7-dibromofluorene (20.0 g, 61.7 mmol), 1-alkylbromide (136 mmol), benzyltriethylammonium chloride (1.0g, 4 mmol) and DMSO (60 mL) were added into a 250 mL flask. 30 mL of 50% NaOH solution was added slowly into this mixture with vigorous stirring with temperature kept below 60 ^{o}C, and the solution was stirred at 60 ^{o}C for 16 h. The solution was then cooled down to room temperature, added with 50 mL of water and was extracted with 100 mL of hexanes. The water layer was separated and extracted with 50 mL of hexanes twice, and the combined organic layer was washed with 50 mL of water twice and dried over $MgSO_4$. The dried solution was passed through a short silica gel column to remove color, and the solvent was removed using a rotary evaporator. The solid residual was purified by washing with 100 mL cold methanol twice and then cold acetone twice, and re-crystallized in acetone to give white crystal. The product with C10 alkyl chain was liquid and was purified by chromatography on silica gels using hexane as eluent.

2,7-dibromo-9,9-didecylflourene (FD-Br_2): 36g, 95%, ^{1}H NMR δ (ppm in $CDCl_3$): 7.51 (2H, d, *J*=8Hz), 7.44 (2H, d, *J*=8Hz), 7.43(2H, s), 1.89 (4H, m), 1.30-1.11(16H, m), 1.11-0.99(12H, m), 0.85 (6H, t, *J*=7.0 Hz), 0.57(4H, M).

2,7-dibromo-9,9-didodecylflourene (FDD-Br_2): 41g, 90%, ^{1}H NMR δ (ppm in $CDCl_3$): 7.51 (2H, d, *J*=8Hz), 7.44 (2H, d, *J*=8Hz), 7.43(2H, s), 1.90 (4H, m), 1.31-1.10(24H, m), 1.10-0.97(12H, m), 0.86 (6H, t, *J*=7.0 Hz), 0.57(4H, M).

2,7-dibromo-9,9-ditetradecylflourene (FTD-Br_2): 37g, 85%, ^{1}H NMR δ (ppm in $CDCl_3$): 7.50 (2H, d, *J*=8Hz), 7.44 (2H, d, *J*=8Hz), 7.43(2H, s), 1.90 (4H, m), 1.32-1.11(32H, m), 1.11-0.98(12H, m), 0.86 (6H, t, *J*=7.0 Hz), 0.57(4H, M).

1-2. 2,7-dibromo-9,9-dioctadecylflourene (FOD-Br_2): 2,7-dibromofluorene (16.2 g, 50 mmol), 1-bromooctadecane (37.0 g, 110 mmol), KI (0.2 g, 1 mmol) and DMSO (100 mL) were added into a 250 mL flask. KOH powder (11.2 g, 200 mmoL) was added slowly into the solution protion by portion with vigorous stirring to keep the temperature below 50 ^{o}C, and the solution

was stirred at 50 ^{o}C for 3 h and then 60 ^{o}C for 30 min. The solution was then cooled down to room temperature, added with 100 mL of water and was extracted with 100 mL of hexanes. The water layer was separated and extracted with 50 mL of hexanes twice, and the combined organic layer was washed with 50 mL of water twice and dried over MgSO4. The dried solution was passed through a short silica gel column to remove color, and the solvent was removed using a rotary evaporator. The solid residual was washed with 100 mL cold methanol twice and then cold acetone twice, and re-crystallized in acetone to give white crystal (32.2g, 78%). ^{1}H NMR δ (ppm in $CDCl_3$): 7.50 (2H, d, *J*=8Hz), 7.44 (2H, d, *J*=8Hz), 7.43(2H, s), 1.89 (4H, m), 1.31-1.10(48H, m), 1.10-0.99(12H, m), 0.87 (6H, t, *J*=7.0 Hz), 0.56(4H, m).

1-3. 9,9-Dialkylfluorene-2,7-bis(pinacolato boron): 2,7-dibromo-9,9'-dialkyllfluorene solution (30.0 mmol) in 300 mL of anhydrous THF was evacuated under vacuum and refilled with argon three times. The solution was cooled down to –78 ^{o}C and was added with 1.6 M n-BuLi (39.4 mL, 63 mmol) dropwise and stirred for 1 h at -40 ^{o}C. The solution was cooled to -78 ^{o}C again and $B(OiPr)_3$ (24g, 128 mmol) was added into the mixture with stirring at this temperature. The reaction mixture was then warmed to RT and stirred for 16 h. 2N HCl was added into the solution at 0 ^{o}C and stirred for 30 min. The separated aqueous layer was extracted with 100 mL ether twice. The combined organic layer was washed with brine (50 mL) three times, dried over $MgSO_4$. The solution was concentrated using rotary evaporator and then was dropped into hexane to precipitate the product. The solid was collect by filtration. After dried under vacuum, it was added into 150 mL of dry toluene. Pinacol (10.6 g, 90.0 mmol) was added into the mixture. The mixture was heated to reflux for 3 hr with the produced water removed using a Dean Stark trap. The solution was washed with 50 mL of water twice, dried over $MgSO_4$ and then the solvent was removed by rotary evaporator. The residual was purified by column chromatography with silica gel use EtOAc/hexane (1/20) followed by a re-crystallization in EtOH to afford white crystal.

9,9-Didecylfluorene-2,7-bis(pinacolato boron) (FD-$Bpic_2$): 14.3 g, 68%. ^{1}H NMR δ (ppm in $CDCl_3$): 7.79 (2H, d, *J*=7.6Hz), 7.73 (2H, s), 7.70 (2H, d, *J*=7.6Hz), 1.98 (4H, m), 1.38 (24H, s), 1.30-1.07 (16H, m), 1.07-0.93(12H, m), 0.85 (6H, t, *J*=7.0 Hz), 0.53(4H, m).

9,9-Didodecylfluorene-2,7-bis(pinacolato boron) (FDD-Bpic$_2$): 16.7 g, 74%. ^{1}H NMR δ (ppm in $CDCl_3$): 7.79 (2H, d, *J*=7.6Hz), 7.73 (2H, s), 7.70 (2H, d, *J*=7.6Hz), 1.98 (4H, m), 1.38 (24H, s), 1.30-1.07 (24H, m), 1.07-0.95(12H, m), 0.85 (6H, t, *J*=7.0 Hz), 0.53(4H, m).

9,9-Ditetradecylfluorene-2,7-bis(pinacolato boron) (FTD-Bpic$_2$): 16.2g, 67%. ^{1}H NMR δ (ppm in $CDCl_3$): 7.79 (2H, d, *J*=7.6Hz), 7.73 (2H, s), 7.70 (2H, d, *J*=7.6Hz), 1.98 (4H, m), 1.38 (24H, s), 1.30-1.07 (32H, m), 1.07-0.95(12H, m), 0.85 (6H, t, *J*=7.0 Hz), 0.53(4H, m).

9,9-Dioctadecylfluorene-2,7-bis(pinacolato boron) (FOD-Bpic$_2$): 22.5g, 81.2%. ^{1}H NMR δ (ppm in $CDCl_3$): 7.79 (2H, d, *J*=7.6Hz), 7.73 (2H, s), 7.70 (2H, d, *J*=7.6Hz), 1.98 (4H, m), 1.38 (24H, s), 1.30-1.07 (24H, m), 1.07-0.94(12H, m), 0.85 (6H, t, *J*=7.0 Hz), 0.53(4H, m).

1-4. Poly(9,9-dialkylfluorene): 9,9-Dialkylfluorene-2,7-bis(pinacolato boron) (5.1 mmol), 2,7-Dibromo-9,9-dioctylfluorene (5.0 mmol) were accurately weighed into a 100 mL flask equipped with a stir bar and a condenser. Toluene (50 mL), 2M Na_2CO_3 solution (20 mL) and ALIQUAT336 (5 drops) were also added into the flask, The system was sealed, degassed under vacuum and filled with argon for three times. Pd(PPh_3)$_4$ (58 mg, 0.05 mmol) was added into the flask in a glove box. The mixture was heated to gentle reflux for 24 h under the protection of argon. The reaction mixture was cooled down to RT, water layer was removed, organic layer was washed with 20 mL water twice and poured slowly into 400 mL of acetone in a beaker with good agitation. The precipitated fiber-like polymer was collected by filtration, washed with 200 mL acetone twice and dried under vacuum.

Poly(9,9-didecylfluorene) (PFD), Mn: 13,600 Da, PDI: 2.7; ^{1}H NMR δ (ppm in $CDCl_3$): 7.82 (2H), 7.66 (4H), 2.11 (4H), 1.30-1.02 (28H, m), 0.82 (6H, t, *J*=7.0 Hz), 0.81(4H).

Poly(9,9-didodecylfluorene) (PFDD), Mn: 21,700 Da, PDI: 4.1; ^{1}H NMR δ (ppm in $CDCl_3$): 7.82 (2H), 7.66 (4H), 2.11 (4H), 1.30-1.02 (36H, m), 0.82 (6H, t, *J*=7.0 Hz), 0.81(4H).

Poly(9,9-ditetradecylfluorene) (PFTD), Mn: 13,400 Da PDI: 3.0; ^{1}H NMR δ (ppm in $CDCl_3$): 7.82 (2H), 7.66 (4H), 2.11 (4H), 1.30-1.02 (44H, m), 0.82 (6H, t, *J*=7.0 Hz), 0.81(4H).

Poly(9,9-dioctadecylfluorene) (PFOD), Mn: 23,700 PDI: 4.2; ^{1}H NMR δ (ppm in $CDCl_3$): 7.82 (2H), 7.66 (4H), 2.11 (4H), 1.30-1.02 (60H, m), 0.82 (6H, t, *J*=7.0 Hz), 0.81(4H).

1-5. TGA and DSC curves: The TGA curves of PFs in Fig. S1a show that the T_d at 1% weight loss is about 370~390 ^oC for these polymers. The residual weight at 650 ^oC is 47.5, 40.9, 37.1, 32.9 and 29.4% for PFO, PFD, PFDD, PFTD and PFOD respectively, showing a good correlation with the polymer structures. This value is about 5% higher than the backbone weight, indicating the weight loss is attributed to the decomposition of the side alkyl groups. DSC curves in Fig. S1b were collected from the 1st heating scan, showing a glass transition temperature (Tg) of 136, 101, 48, 40 and 35 ^oC for PFO, PFD, PFDD, PFTD and PFOD, respectively.

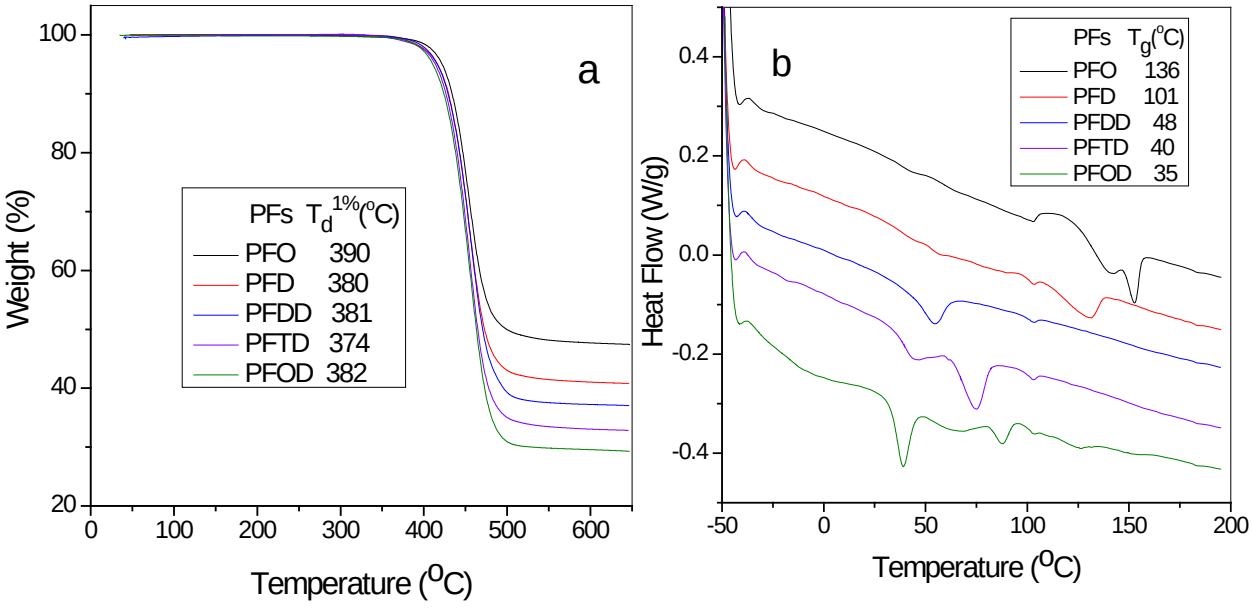

Fig. S1. TGA and DSC curves of polyfluorenes measured under N_2 at a heating rate of 10 ^oC/min, DCS curves were taken from the 1st heating scan.

2. Estimation of nanotube content of the raw laser SWCNTs by TGA:

Nanotube content of the raw laser-derived SWCNTs was estimated form TGA measurement (Fig. S2): This test was conducted in CO_2 flow (50 mL/min), where two distinguished decomposition stages were observed in ranges of 300~600 and 600~1000 ^oC corresponding to amorphous carbon and SWCNTs, respectively. 53% weight loss was observed in the SWCNT decomposition stage.

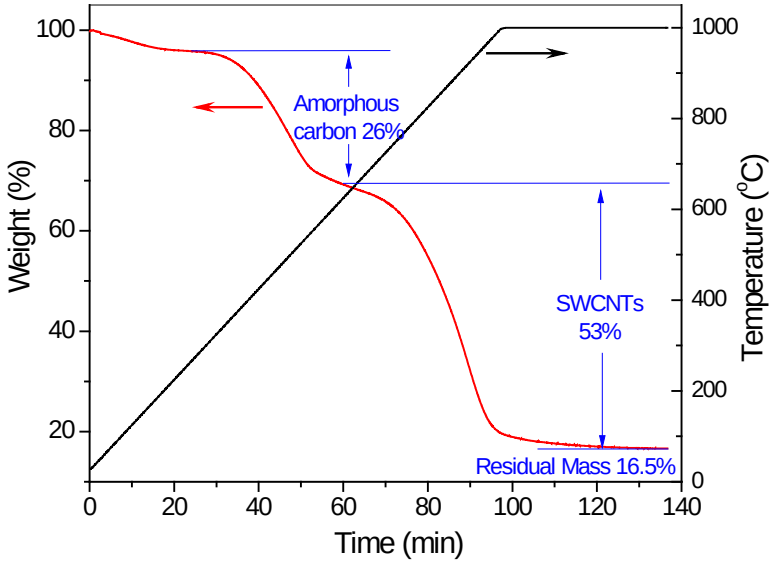

Fig. S2. TGA curve of the raw laser SWCNTs at a rate of 10 ^{o}C/min from RT to 1000 ^{o}C followed by an isothermal stage of 40 min under a CO_2 flow (50 mL/min). It was done following a reported method [2]. The first major weight loss stage is mainly related to the decomposition of amorphous carbon and the second stage is mainly attributed to the decomposition of SWCNTs.

3. **Yield and SWCNT concentration measurement using absorption spectroscopy.**

Yield is one of the two most important performance data other than purity for the enrichment process. It is expressed as the mass percentage of the sc-SWCNTs after enrichment relative to the total mass of SWCNTs present in the starting material. The latter was calculated from the TGA analysis as described above. Principally, yield can be obtained by comparing the weight of sc-SWCNTs in the final product of the enrichment with the weight of starting material. But the final product is polymer wrapped SWCNTs and therefore it is a mixture of polymer and SWCNTs. The polymer content in the final product has to be detected in order to evaluate the sc-SWCNT yield. The study by spectroscopic approach as described in Ref 2 shows a more convenient method to simultaneously determine both of the polymer and sc-SWCNTs in the final product. Therefore, we calculate polymer and SWCNT concentration (mg/mL) of the enriched dispersions from their absorption spectra as demonstrated in Fig.S3, and then the yield of the enrichment can be deduced from this result.

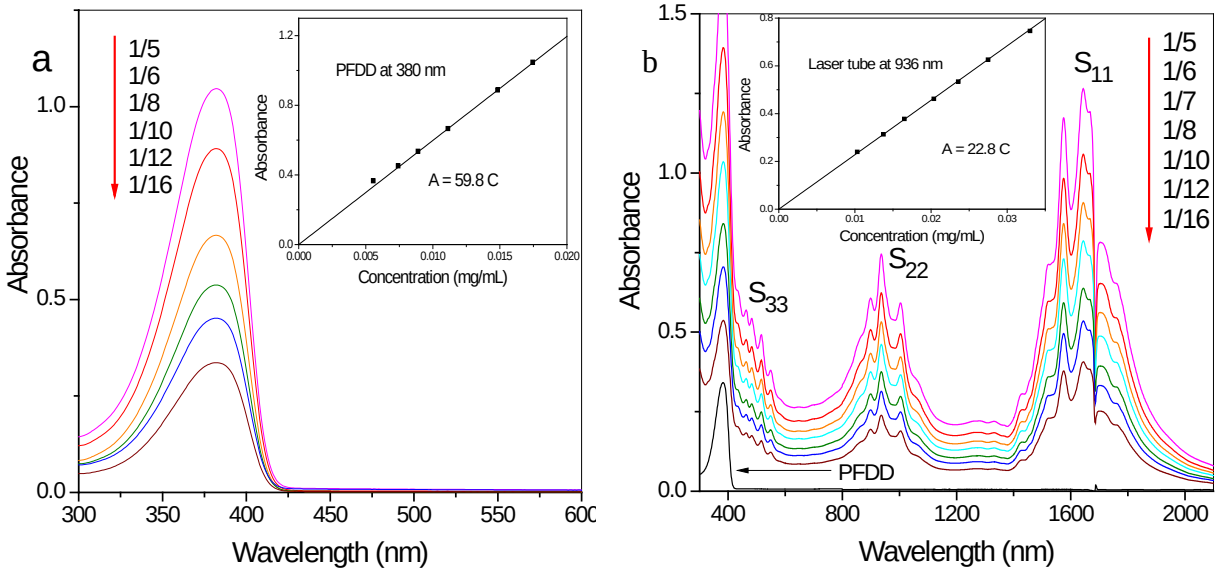

Fig. S3, Absorption spectra (a) of the diluted PFDD solution (0.089 mg/mL) in toluene by a factor of 5, 6, 8, 10, 12 and 16; and (b) of the enriched laser sc-SWCNT (Fig. 1-0.5) solution (0.165 mg/mL) diluted by a factor of 5,6,7,8,10,12, and 16.

From the absorption spectrum of the enriched product, such as that shown in Fig. S3b, we can see that the polymer (PFDD) only has a single peak at 380 nm, and sc-SWCNT shows three absorption bands in the regions of 1400-1900 nm for S_{11}, 700-1100 nm for S_{22} and 450-550 nm for S_{33}. All these bands and the PFDD peak are well separated. This feature allows us to use Beers law ($A=\varepsilon lc$) to correlate the peak absorbance (A) and the concentration of polymer and sc-SWCNTs (c in mg/mL) through the extinction coefficient (ε in mL/mg.cm), where l is the path length in cm and is 1 cm in this work. The extinction coefficient of the polymer at 380 nm (ε_{380}) and the sc-SWCNTs at 936 nm (ε_{936}) was determined from the pure polymer and from a highly purified sc-SWCNT sample (Sample 0.5 of Fig. 1 in the main text), with sc-purity over 99% as will be shown in the following discussion. Therefore, 0.89 mg of PFDD was dissolved in 10 mL of toluene and the absorption spectra of its diluted solutions (by factors of 5, 6, 8, 10, 12 and 16) were collected and displayed in Fig. S3a with the plot of absorbance at 380 nm vs. concentration inserted. The linear best fit line of this plot gives the extinction coefficient of the polymer (ε_{380}) of 59.8 mL/mg.cm. A similar work on 1.65 mg of the enriched sc-SWCNT sample as shown in

Fig. S3b resulted in an apparent extinction coefficient at 936 nm of the enriched nanotube samples of 22.8 mL/mg.cm. We call this value apparent extinction coefficient due to the sample being a mixture of polymer and nanotubes. Therefore the polymer influence has to be eliminated from this value. This was done by a similar analysis of the absorbance at 380 nm of Fig. S3b. Because the PFDD absorption peak at 380 nm is overlapped with a background signal of the nanotubes and thus the absorption at 380 nm for PFDD (dA_{380}) is estimated as shown in Fig. S4. The plot of dA_{380} vs. concentration of this sample gives an apparent extinction coefficient at 380 nm of 31.6 mL/mg.cm. Comparison of this value with ε_{380} of the pure PFDD (59.8 mL/mg.cm) yields a 52.8% PFDD content of this sample. Therefore the extinction coefficient of the enriched laser SWCNT should equal to 22.8/(1-0.528) = 48.3 mL/mg.cm. It should be noted that this value is slightly higher than the extinction coefficient of the purified laser SWCNTs reported in Ref 2 (41.1 mL/mg.cm), where amorphous carbon was removed yet m- and sc-SWCNTs remained. This difference is understandable when we take the m-SWCNT in Ref 2 as impurity for the sc-SWCNT extinction coefficient calculation.

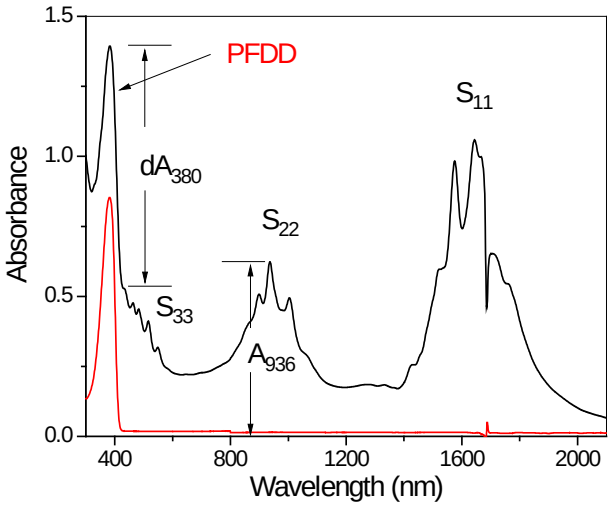

Fig. S4. Absorption spectra of PFDD and PFDD enriched laser sc-SWCNTs, the absorbance calculation of the PFDD peak at 380 nm (dA_{380}) and the S_{22} peak at 936 nm (A_{936}) was indicated.

4. Semiconducting (sc-) purity assessment by absorption peak ratio.

The sc-purity of the enriched sc-SWCNTs is the key factor to determine the TFT device performance. Unfortunately, it has remained an issue to quantitatively measure the sc-purity to

date. As can be seen in Fig. 1 in the main text, the laser tubes possess absorption peaks in several wavelength regions for sc-tubes (S11 in 1400-1900 nm, S22 in 750-1150 nm, S33 in 420-580 nm) and for m-tubes (M11 in 600-750 nm). This feature was also observed for the other large-diameter SWCNTs such as arc-discharge and plasma tubes. Based on this property, Nanointegris estimated the sc-SWCNT purity of one of their product (IsoNanotubes-99) enriched by DGU to be 99% by comparing the integrated areas of the S22 and M11 peak envelops. However, this method is not suitable for the product with a higher purity as shown in Fig. 1 in the main text, when the purity increase beyond a certain level, the M11 peak at 646 and 696 nm does not appear anymore, while the background intensity in this region continues to decrease as the impurities including m-tubes were further removed. Under this circumstance, Blackburn in one of his recent papers compared the UV spectrum of their sample with that of IsoNanotubes-99, and find their enriched sample has a deeper valley between the S22 and S33 bands. [2] Therefore, they conclude an equivalent or higher sc-purity of their sample. Using the same strategy, we also compare the absorption spectrum of our sample shown in Fig. 1 (0.5) in the main text with the spectra of Blackburn sample in Fig. S5. For a reasonable comparison, the spectra were normalized based on the S22 band. It is showed that this sample has better resolved S22 peaks and comparable or slightly deeper background intensity in this region, indicating a comparable sc-purity.

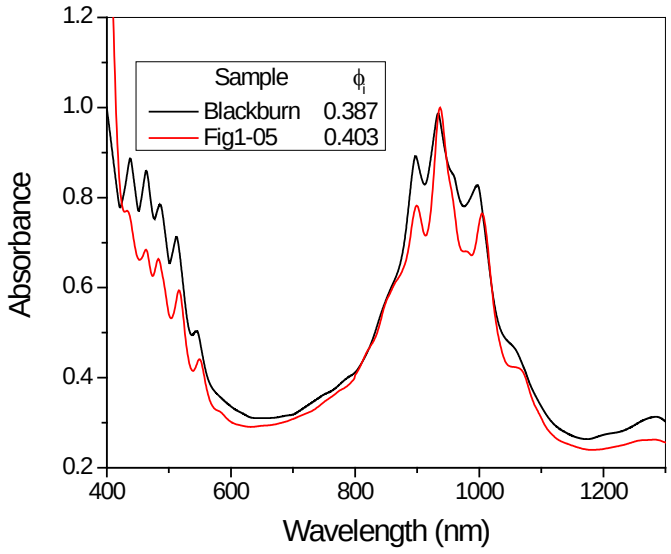

Fig. S5. Comparison of the absorption spectrum (Fig. 1-0.5) with the spectrum of the Blackburn's sample. For a reasonable comparison, the spectra were normalized based on the S22 band. The curve for Blackburn's sample is re-plotted from Fig. S8 of Ref 2.

However, this kind of comparison is not convenient for a quick evaluation of the sc-purity. Therefore we attempt to derive a metric from the absorption spectrum for this purpose. As shown in Fig. 1 in the main text, the enrichment not only removed the M11 absorption band, but also significantly reduced the background intensity in the M11 and S22 region. Because the absorption background was mainly contributed by the featureless absorption of amorphous carbon, [2-5] the integrated area of the M11 and S22 peak envelop comparing to the total area in this region should be correlated with the SWCNT content in the sample. Therefore, Curve 8.0 of Fig. 1 in the main text was taken as an example and was re-plotted with absorbance vs. energy expressed as wavenumber in Fig. S6, from which absorption peak ratio ($\phi_i = A_{CNT}/(A_{CNT} + A_B)$) is defined, where A_{CNT} was the enveloping area of the M11 and S22 bands enclosed by the linear baseline (pink area) in the region from 8400 to 16000 cm^{-1} (1900-625 nm), attributing to the nanotubes, and A_B was the area covered by the linear baseline of the same region, attributing mostly to the amorphous carbon. A similar model covered only S22 region was originally proposed by Itkis for evaluating the nanotube content of pristine SWCNT products, [5] This value for most as-prepared SWCNT samples were found to be low. As the SWCNT content *vs* amorphous carbon increases, it increases and approaches a maximum value of 0.325 for the pure SWCNT samples. [3] However, our work will show that the SWCNT peak ratio (ϕ_i) will reach a higher value for highly semi-conducting enriched samples and thus the Itkis model is not applicable in this work. This is because that the removal of the M11 peak due to the elimination of m-SWCNTs removes the overlap between the S22 and M11 absorption features, which results in a lower background intensity in this region, and thus lead to a small A_B value and a higher ϕ_i ratio. This feature in reverse makes ϕ_i very sensitive to the m-SWCNT content in an enriched sample. Consequently, ϕ_i was adopted here to evaluate the sc-purity of the enriched samples, where a large value is more reflective of the variation in semiconducting/metallic content in high sc-purity samples as opposed to tube content vs non-tube carbon. The integrations of the absorption curves of Fig 4-0.5 and Blackburn's sample in the range of 8400-16000 cm^{-1} (1190-

625 nm) give 0.403 and 0.387 of the ϕ_i ratios for these two samples. This result agrees well with that from the absorption spectra as discussed above.

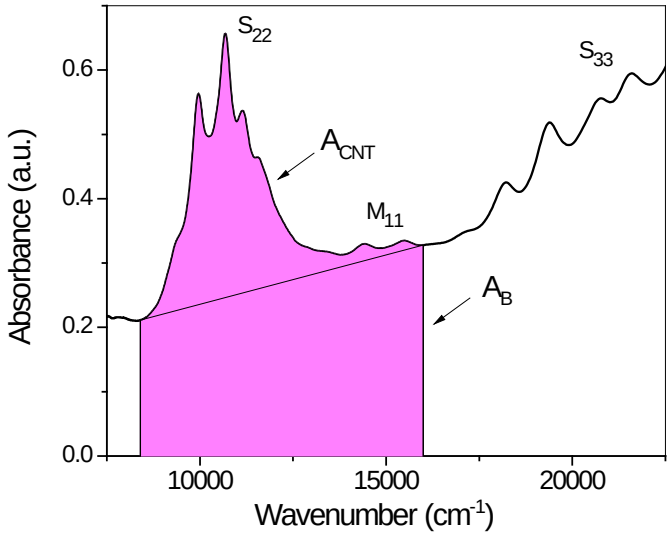

Fig. S6. Schematic illustration of the definition of the SWCNT peak ratio ($\phi_i = A_{CNT}/(A_{CNT} + A_B)$), where A_{CNT} is the enveloping area of the M11 and S22 bands enclosed by the linear baseline (pink area) corresponding to the amount of m- and sc-SWCNTs in the sample, and A_B was the area covered by the linear baseline of the same region, mainly attributing to the amorphous carbon impurity.

5. Polymer side chain length effect.

PFD (C10), PFDD (C12), PFTD (C14), and PFOD (C18) have been tested for SWCNT extraction at a SWCNT concentration of 0.5 mg/ml and a polymer/SWCNT ratio of 0.8 in toluene. The absorption spectra of the enriched sample were compared in Fig. S7. It showed that the nanotubes enriched by PFD, PFDD, PFTD and PFOD gave a similar absorption spectrum with a yield (η) of 5.3%, 6.8%, 5.4% and 6.4%, and absorption peak ratios (ϕ_i) of 0.416, 0.403, 0.410 and 0.404, respectively under the conditions described in the figure caption. This result proves that these four polymers are highly effective to disperse and extract sc-SWCNTs.

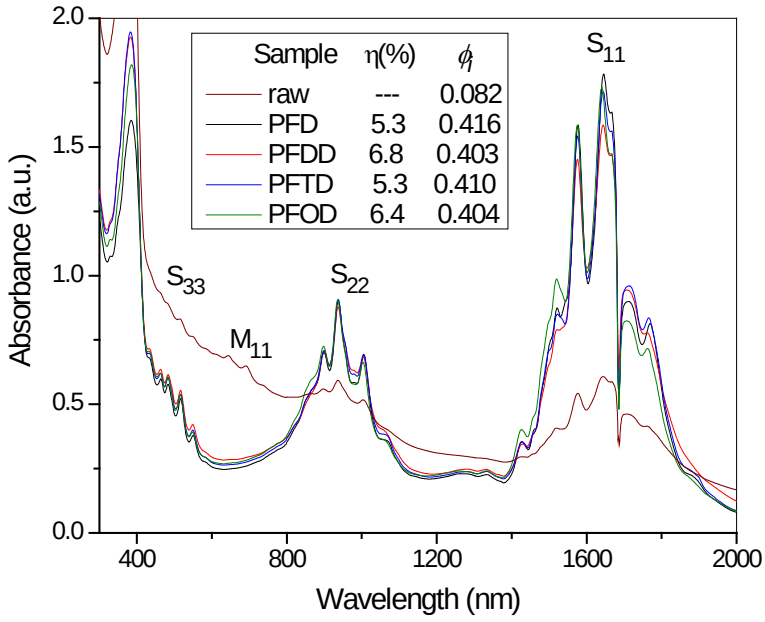

Fig. S7. Absorption spectra, yield (η) and ϕ_i ratio of the products from the extraction by PFD, PFDD, PFTD and PFOD at a concentration of 0.5 mg/ml, and a polymer/SWCNT ratio of 0.8 in toluene. The spectrum of the raw materials from the PFDD dispersion before centrifugation was also plotted for comparison. For a better comparison, the spectra of the enriched samples were normalized at 936 nm.

6. PLE mapping analysis.

PLE map of the sample in Fig. 4 in the main text showed about 19 (n,m) species in the spectrum, in which about 8 or 9 having peak intensities higher than or close to 0.5. All these chiralities are located in a small area in the index family (Fig. S8) with the major 9 chiralities in a narrow diameter range from 1.25-1.35 nm (blue area). The PL emission and excitation slices of the PLE map (Fig. 4 in main text) were integrated and the resulting curves were superimposed with the absorption spectrum in Fig. S9. For the sum of emission slices, there is a one to one correspondence with the E_{11} absorption, as expected under the assumption there is a negligible amount of energy transfer between nanotubes in the solution. In other words, the absorption and emission signals are dominated by individualized nanotubes, indicating the bundling is weak if at all present in the dispersion.

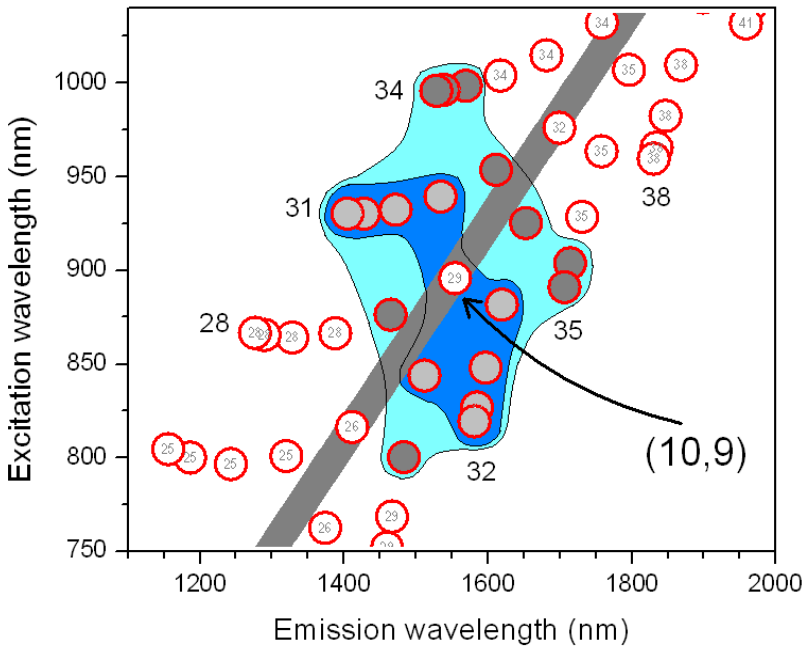

Fig. S8: Chirality map of S_{22} versus S_{11} wavelengths. The two shaded areas show chiralities with a diameter distribution between 1.25 and 1.35 nm (blue), and between 1.20 and 1.40 nm (cyan). The number of possible chiralities is 9 and 19, respectively. The indicating numbers are 2n+m of the nanotubes.

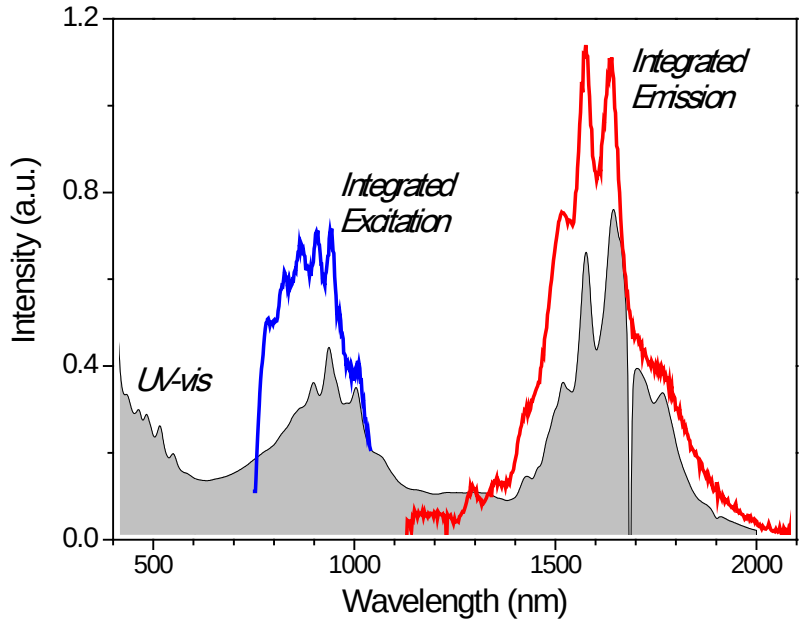

Fig. S9. Absorption spectrum (shaded gray) and extracted data from the PLE map in Fig. 4 of the enriched sc-SWCNTs. The blue line represents the excitation curve and the red line represents the emission curve extracted from the PLE map.

7. TEM and SEM Evaluation of the enriched sc-SWCNTs.

The length of the enriched nanotubes was evaluated by TEM and SEM with the images displayed in Fig. S10. The TEM image (Fig. S10a) shows straight individual nanotubes with few bundles. A number average length of 1.3 µm (length average, 1.8 µm) was measured from about 200 nanotubes in the SEM image (Fig. S10b). This sample was prepared by depositing a drop of highly diluted solution on a silicon wafer followed by rinsing with toluene. It can be seen that most tubes were individually dispersed.

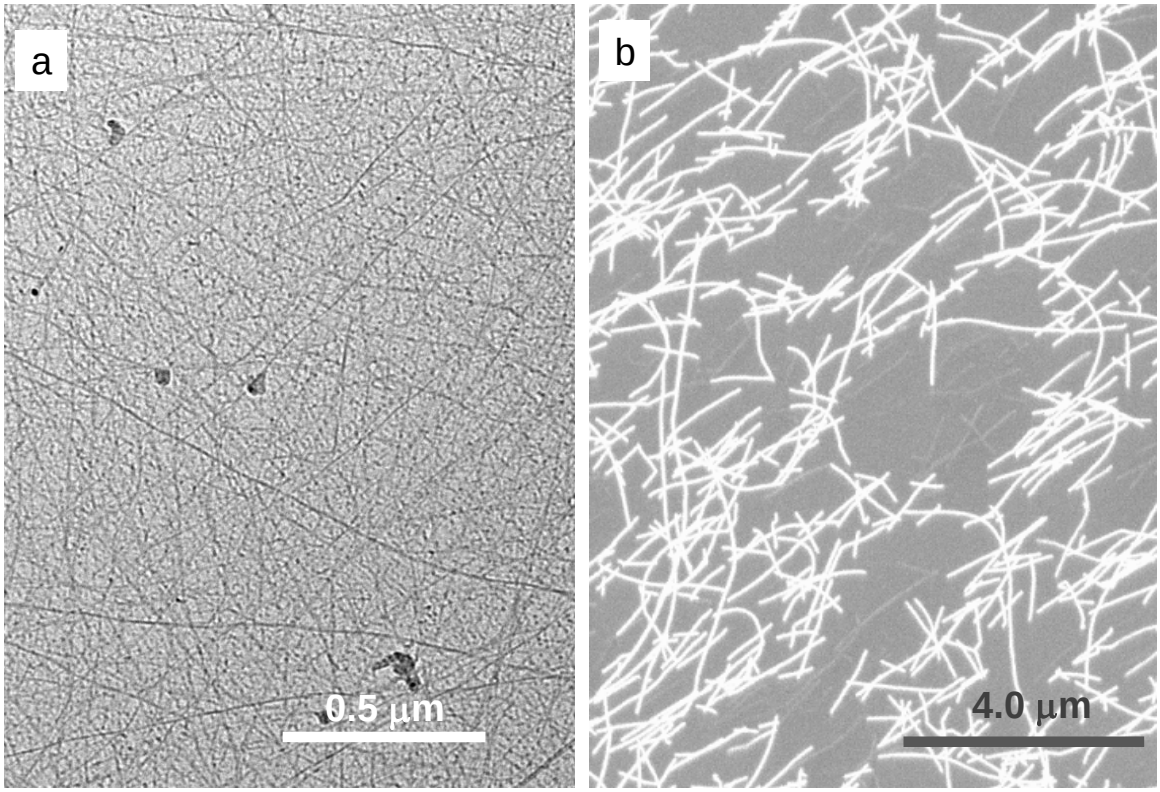

Fig. S10. TEM (a) and SEM (b) images of enriched sc-SWCNTs. The TEM sample was prepared by placing a drop of diluted nanotube solution in toluene on a carbon coated copper grid with the

excess solution removed using a piece of filter paper. The SEM sample was coated on a SiO_2/Si substrate with a drop of diluted solution followed by rising with toluene.

The layout of the 25 devices on the chip and the SEM image of the nanotube networks in 4 representative devices were displayed in Fig. S11. It showed the mobility varied from 5 to 43 $cm^2V^{-1}s^{-}1$ of the 25 devices. But no apparent difference in tube density was observed from the SEM image of the nanotube networks in the devices at different location.

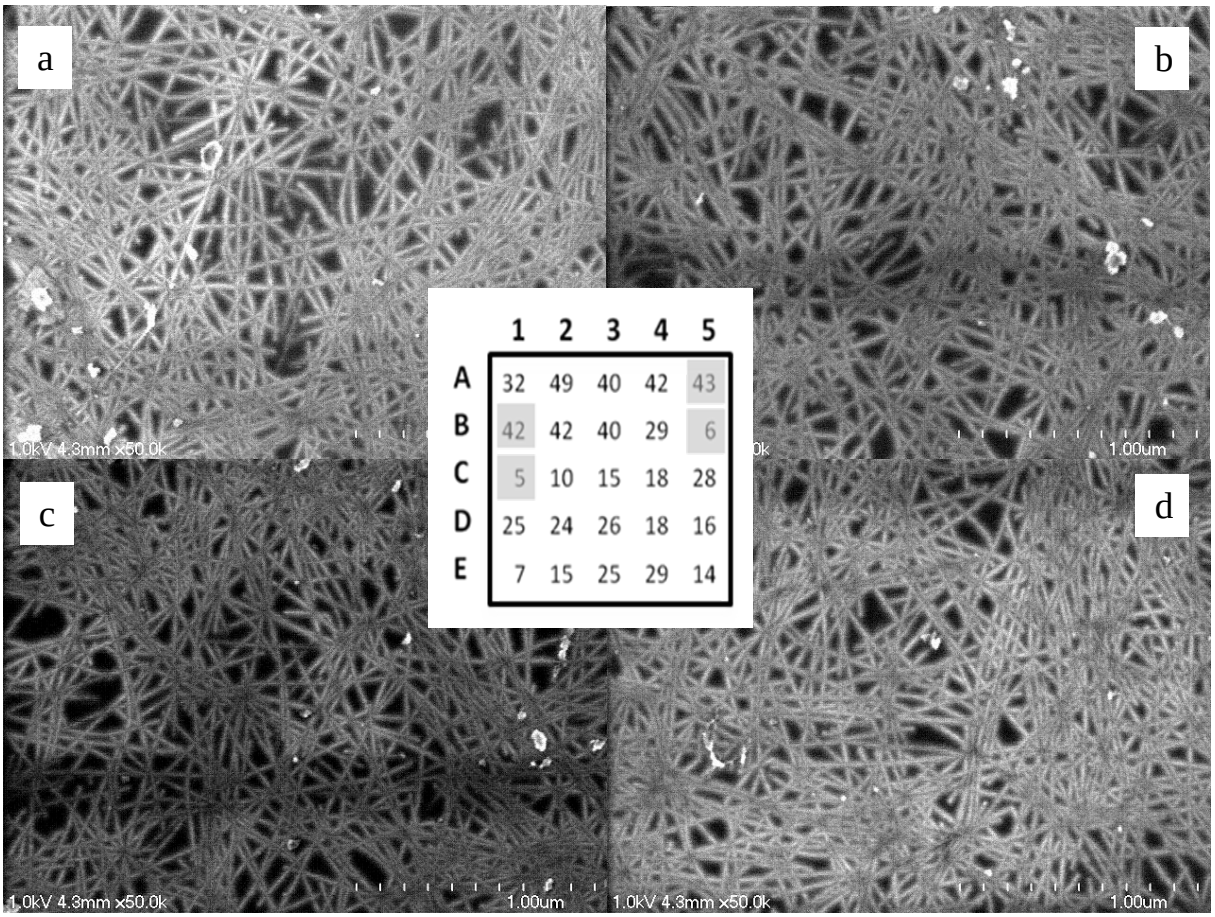

Fig. S11. SEM images of the nanotube networks formed in the representative devices (a) device A5 with mobility of 43 $cm^2V^{-1}s^{-1}$), (b) device B1 with mobility of 42 $cm^2V^{-1}s^{-1}$, (c) device B5 with mobility of 6 $cm^2V^{-1}s^{-1}$, and (d) device C1 with mobility of 5 $cm^2V^{-1}s^{-1}$, and the layout of the 25 devices on the single chip and their corresponding mobility values (inset).

References:

1. N. Berton, F. Lemasson, J. Tittmann, N. Sturzl, F. Hennrich, M. M. Kappes and M. Mayor, *Chem. Mater*., 2011, **23**, 2237–2249.

2. K. S. Mistry, B. A. Larsen and J. L. Blackburn, *ACS Nano*, 2013, **7,** 2231–2239.

3. M. E. Itkis, D. E. Perea, R. Jung, S. Niyogi and R. C. Haddon, *J. Am. Chem. Soc.*, 2005, **127,** 3439-3448.

4. A. V. Naumov, S. Ghosh, D. A. Tsyboulski, A. M. Bachilo and R. B. Weisman, *ACS Nano,* 2011, ***5,*** 1639-1648.

5. M. E. Itkis, D.E. Perea, S. Niyogi, S. M. Rickard, M. A. Hamon, H. Hu, B. Zhao and R. C. Haddon, *Nano Lett*., 2003, **3,** 309-314.